


Solubility of Acetone-Methanol Mixtures in Matrimid Glassy Polymer: Experimental Data and Modelling through NET-GP and PC-SAFT

Lorenzo Merlonghi, Ferruccio Doghieri, Marco Giacinti Baschetti^{*} 

Department of Civil, Chemical, Environmental and Material Engineering, (DICAM), Alma Mater Studiorum – Università di Bologna, via Terracini 28, 40131 Bologna, Italy

ARTICLE INFO

Keywords:

Liquid solubility in polymer
Polymer solvent equilibrium
Glassy polymers modelling (NET-GP)
Ternary mixtures
PC SAFT Equation of State

ABSTRACT

In this work, the PC-SAFT equation of state and the NET-GP approach have been considered for the description of the thermodynamic equilibrium between liquid acetone-methanol mixture and Matrimid glassy polymer. Pure component parameters of the PC-SAFT EoS for the system under consideration were retrieved from literature and checked by predicting the vapor pressure and saturated molar volumes of both Methanol and Acetone. Considering the binary mixture, isothermal VLE data at 35°C were fitted by using PC-SAFT, in order to derive binary interaction coefficients, the latter then proved to be able to correctly describe also the volume of the liquid mixture at 35°C and 1 bar. Considering the binary Acetone-Matrimid and Methanol-Matrimid systems, binary interaction and swelling coefficients needed for the description of the glassy phase were retrieved by fitting pure component vapor sorption isotherms at 35°C through the NET-GP approach coupled with PC-SAFT equation of state. Finally, based on the parameters obtained from the binary mixtures, the ternary Acetone-Methanol-Matrimid system at 35°C and 1 bar was predicted, without using additional parameters. The results were compared with experimental data related to liquid sorption in the polymer as obtained by coupling FTIR-ATR analysis and gravimetric methods. The agreement was remarkable testifying to the ability of the proposed approach to describe sorption of binary mixtures involving hydrogen bonding compounds in glassy polymers.

1. Introduction

Glassy polymer films are widely used for different technical applications like membrane separation processes [1,2], sensors [3,4], packaging [5,6] and medical devices [7]. In most of these applications, the polymeric matrix interacts with different chemical species, and such interactions may affect thermo-mechanical properties and stability of the polymer. For this reason, it is important to have a tool able to evaluate these kinds of interactions and their effects on the polymer properties, in order to increase the lifetime of the products. The main physical properties which allow to characterize the interactions between polymer and environment, are the solubility and the diffusivity of the different penetrants in the polymer phase, considering also possible swelling effects caused by the stress distribution associated with mass transport [8,9]. Polyimides are synthetic glassy polymers characterized by high chemical, mechanical, and thermal stability, due to the high glass transition temperature [10,11,12,13,14]. Being solvent resistant and providing good selectivity, nanoporous polyimide membranes can be used for organic solvent nanofiltration (OSN) processes [15,16].

However, in some kinds of polyimides, the organic solvents induce swelling phenomena in the polymer matrix, leading to density reduction and structure deformation, with respect to the dry material. In particular, the glass transition temperature and the density can be reduced by the presence of highly soluble penetrants. As a result, the structural conformation of the polymer can change, from a glassy to a rubbery state, affecting all the properties (mechanical, thermal and barrier) of the material [17,18]. These changes are often deeply connected by the amount of solvent which is able to penetrate the polymer, which can be measured and modelled using different approaches [19].

A wide range of techniques can be used to perform sorption experiments of liquids and vapors in polymers, which however are mainly focused on the analysis of pure component sorption [20,21]. For liquid solvents, the simplest technique is the blot and weight method, based on the measurement of the mass uptake at equilibrium using a simple analytical balance, while for gases and vapors, both volumetric methods like pressure decay and gravimetric methods such as quartz spring balance can be used [22]. Considering gas mixtures, the measurements of the overall sorbed amount must be coupled with a gas concentration

^{*} Corresponding author.

E-mail address: marco.giacinti@unibo.it (M. Giacinti Baschetti).

measurements, such as gas chromatographic techniques, in order to obtain the solubility of each penetrant in the polymer phase [23,24,25,26]. On the other hand, FTIR-ATR technique has proven a powerful technique that can be used to measure the sorbed amount of each species of a mixture in both liquid or vapor phase [27,28,29] as well as polymer swelling upon sorption [30]. However, while pure component sorption data can be easily found in literature, multicomponent sorption data in glassy polymers are still limited in the literature, due to the difficulty in the measurement techniques. For this reason, a modelling strategy able to predict multicomponent sorption based on pure component sorption experimental data is an interesting object of study, especially in systems in which different components can associate, for example through hydrogen bonding.

Concerning the thermodynamic models available for the description of the solubility isotherms of pure fluids in polymers, equations of state (EOS) like the ones based on activity coefficients models such as Flory-Huggins (FH) theory [31,32] and others based on statistical theories such as Lattice Fluid (LF) [33,34,35,36] and Statistical Associating Fluid Theory (SAFT) [37,38], are only able to describe equilibrium systems like rubbery polymeric phases. Considering glassy polymers, empirical models like dual mode sorption, can be used to describe only a few types of solubility isotherms [39,40], while other approaches like the Non-Equilibrium Thermodynamics for Glassy Polymers (NET-GP) can be used to describe a wide range of solubility isotherms [22,41,42,43,44,45,46]. This latter approach takes the expression of the Helmholtz free energy from a classical EOS for polymers but uses the polymer density as an internal state variable of the system, to obtain the corresponding non-equilibrium model. By using this approach, non-equilibrium glassy polymers can be described relying on a suitable EOS able to describe the equilibrium properties, by using the same pure component parameters and adding only a further parameter needed to describe the density of the non-equilibrium polymer.

Pure component parameters are available in literature for different classes of organic penetrants but are sometimes difficult to retrieve for uncommon polymers. For light molecules, they are commonly obtained from pressure–volume–temperature (pVT) and/or vapor-liquid equilibrium (VLE) data. For polymers, on the other hand, they are obtained from pvT data [47,48] and/or liquid-liquid equilibrium (LLE) data [49,50]. Depending on the strategy used, different sets of parameters can be obtained for the same polymer or solvent, which in turn results in a high number of possible combinations in multicomponent systems. In this concern, while the NET-GP approach was widely used to describe pure component sorption in glassy polymers, the same approach was seldom extended to mixture and generally limited only to non-associative gaseous mixtures as in the work by Ricci *et al.* [24,48,51]. To the best of our knowledge, however, it was never used for organic liquid and vapor mixtures with associative components. For such systems, indeed, only a modification of the general non-equilibrium model, based on the dry glass reference perturbation theory (DGRPT), was proposed very recently by Marshall *et al.* [52,53].

Therefore, since the description of multicomponent associative non-equilibrium systems based on the original NET-GP approach is still lacking in the literature, a strategy is proposed for the first time in this work, in which the description of a ternary associative system is performed by using the NET-GP approach, with the PC-SAFT [49,50,54,55,56] as reference EOS, in order to account for molecular associations such as hydrogen bonding.

The ternary system acetone-methanol-Matrimid is chosen as reference system, because solubility isotherms at 35°C were available in the literature for the systems acetone-Matrimid and methanol-Matrimid [22] as well as LVE data for the system acetone-methanol at the same temperature [57]. Moreover, acetone and methanol are organic solvents widely used in industry. Acetone with methanol forms a homogeneous minimum-boiling azeotrope which is not separable by conventional distillation processes. Different methods can be used, such as extractive distillation in the presence of a selective solvent, such as water or

another solvent with a higher boiling point [58,59], or pressure swing batch distillation [60]. Concerning the ternary acetone-methanol-Matrimid system, novel experimental data regarding multicomponent liquid sorption at 35°C and 1 bar are presented in this work, obtained by coupling FTIR-ATR and gravimetric techniques, and used in order to validate the model prediction.

2. Model Description

In the present work, the PC-SAFT model is coupled with the NET-GP approach to describe the thermodynamic properties of the mixtures formed by the different penetrants with the polymer. An accurate description of the PC-SAFT model can be found in the original works by Gross and Sadowski [54,55,56], while a detailed description of the NET-GP approach can be found in the original works by Sarti and Doghieri [41,42]. The main features of the two models are, however, also briefly recalled here for the sake of clarity.

2.1. Pure Components Parameters

In the SAFT framework, molecules are considered as chains of spherical segments. The molecules can be divided into non-associating and self-associating components. A non-associating fluid is completely characterized by three molecular parameters: the number of segments per chain m , the reduced depth of pair potential ϵ/k in K, and the temperature-independent segment diameter σ in Å. For associating fluids, according to the association scheme and the number of associating sites per molecule, two other parameters are required: the reduced association energy of interaction between site A and site B ϵ^{AB}/k in K and the volume of interaction between site A and site B k^{AB} . The PC-SAFT characteristic parameters for penetrants and polymers considered in this work are reported in Table 1, where also the hydrogen bonding sites for the different molecules are presented. In particular, methanol is considered a self-associating fluid with the 2B association scheme. According to this scheme, 2 association sites per molecule are present, one electron donor and one electron acceptor, corresponding to the hydroxyl group of methanol [55]. On the other hand, acetone is considered a non-associating fluid [61], able to form induced associations with methanol according to the same scheme and with the same number of sites, corresponding to the carbonyl group. In particular, the same value of k^{AB} of methanol was used, while ϵ^{AB}/k was kept equal to zero in order to allow cross-association between the carbonyl group of acetone and the hydroxyl group of methanol [62]. Finally, Matrimid is modelled as acetone, with cross-associations with methanol, using the same scheme, with 10 association sites (2 for each carbonyl group) in the repeating unit [50].

2.2. Mixing Rules

Parameters representative of the mixture properties can be easily calculated from the corresponding pure component values, by using different mixing rules. The mean segment number of the mixture \bar{m} is obtained from pure components segment numbers m_i as a linear function of the mole fractions z_i :

$$\bar{m} = \sum_i z_i m_i \quad (1)$$

The parameters for a pair of unlike segments are obtained by conventional Berthelot-Lorentz combining rules [56]:

$$\sigma_{ij} = \frac{1}{2} (\sigma_i + \sigma_j) \quad (2)$$

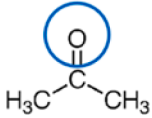
$$\epsilon_{ij} = (1 - k_{ij}) \sqrt{\epsilon_i \epsilon_j} \quad (3)$$

Where k_{ij} is a binary interaction parameter, which can be used to correct the interaction energy between two species in a mixture. On the

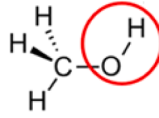
Table 1
PC-SAFT pure components parameters used in this work.

	σ (Å)	m	ϵ/k (K)	k_{AB}	ϵ_{AB}/k (K)	Ref.
Matrimid	3.1	3040	320	0.035176	0	[50]
Acetone	2.77409	3.2557	253.406	0.035176	0	[61]
Methanol	1.5255	3.2300	188.90	0.035176	2899.5	[55]

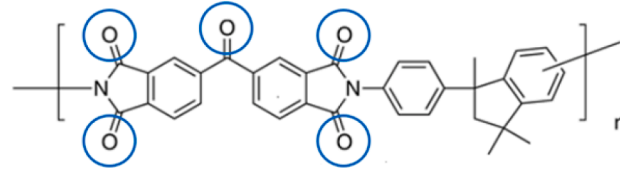
Hydrogen Bonding Sites*



Acetone



Methanol



Matrimid

* Red circles refer to self-associating sites, while blue ones refer to sites forming induced associations only.

other hand, simple combining rules for cross-association were suggested by Wolbach and Sandler [63], in which a binary interaction parameter ν_{ij} is used to correct the association energy between two species in the mixture.

$$\epsilon^{A_i B_j} = (1 - \nu_{ij}) \frac{1}{2} (\epsilon^{A_i B_i} + \epsilon^{A_j B_j}) \quad (4)$$

$$k^{A_i B_j} = \sqrt{k^{A_i B_i} k^{A_j B_j}} \left(\frac{\sqrt{\sigma_i \sigma_j}}{\sigma_{ij}} \right)^3 \quad (5)$$

2.3. Equilibrium Systems

The original PC-SAFT model was developed in order to describe the behaviour of simple and complex fluids, when they are in thermodynamic equilibrium. In this model, the reduced residual Helmholtz free energy \tilde{a}^{res} is expressed as a function of temperature T , molar density ρ , and composition in each phase z_i , as the sum of three major contributions. The sum of the repulsion-dispersion contribution typical of individual segments \tilde{a}^{seg} , the contribution due to the fact that these segments can form a chain \tilde{a}^{chain} , and the contribution due to the possibility that some segments form association complexes with other molecules \tilde{a}^{ass} , lead to the following expression:

$$\tilde{a}^{\text{res}}(T, \rho, z_i) = \tilde{a}^{\text{seg}}(T, \rho, z_i) + \tilde{a}^{\text{chain}}(T, \rho, z_i) + \tilde{a}^{\text{ass}}(T, \rho, z_i) \quad (6)$$

Once \tilde{a}^{res} is calculated as a function of T , ρ and z_i all other thermodynamic properties can be easily evaluated using well known thermodynamic relationship, to give a complete description of an equilibrium systems. In particular, the compressibility factor Z is calculated as:

$$Z = 1 + \rho \left(\frac{\partial \tilde{a}^{\text{res}}}{\partial \rho} \right)_{T, z_i} \quad (7)$$

while, the pressure is obtained as a function of T , ρ , Z and gas constant R :

$$p = Z\rho RT \quad (8)$$

Finally, the fugacity coefficient of each species in the mixture ϕ_i is calculated as:

$$\ln(\phi_i) = \left(\frac{\partial \tilde{a}^{\text{res}}}{\partial \rho_i} \right)_{T, \rho_{j \neq i}} - \ln(Z) \quad (9)$$

2.4. Extension to Non-Equilibrium Systems

In the present work, the NET-GP approach is combined with PC-SAFT in order to describe vapor and liquid solubility in glassy polymers, which are known to be non-equilibrium systems and therefore cannot be simply described by the relationships reported above in Eqs. 6 to 9. The main assumption of the model is that the expression of the Helmholtz free energy in a non-equilibrium system remains substantially the same

as the one in equilibrium [41,42]. In other words, Eq. 6 is still valid for a non-equilibrium system, but its molar density cannot be related to temperature and pressure through an equation of state (Eqs. 7,8) but it is assumed to be dependent on an internal state variable, such as the polymer density in the glassy state. In this sense, the non-equilibrium molar density ρ^{NE} is expressed as a function of the polymer molar density ρ_{pol} and the molar fraction of the polymer s_{pol} trough:

$$\rho^{\text{NE}} = \frac{\rho_{\text{pol}}}{s_{\text{pol}}} \quad (10)$$

Considering this approach, the non-equilibrium reduced Helmholtz free energy $\tilde{a}^{\text{res,NE}}$ is calculated as function of temperature, non-equilibrium molar density ρ^{NE} and molar composition s_i trough:

$$\tilde{a}^{\text{res,NE}}(T, \rho^{\text{NE}}, s_i) = \tilde{a}^{\text{seg,NE}}(T, \rho^{\text{NE}}, s_i) + \tilde{a}^{\text{chain,NE}}(T, \rho^{\text{NE}}, s_i) + \tilde{a}^{\text{ass,NE}}(T, \rho^{\text{NE}}, s_i) \quad (11)$$

As a consequence, once $\tilde{a}^{\text{res,NE}}$ is calculated as a function of T , ρ_{pol} and s_i all other thermodynamic properties can be easily evaluated to give a complete description of the non-equilibrium system. In particular, the compressibility factor of the non-equilibrium phase is calculated as:

$$Z^{\text{NE}} = \frac{p}{\rho^{\text{NE}} RT} \quad (12)$$

The fugacity coefficient of each component in the non-equilibrium phase ϕ_i^{NE} is calculated as:

$$\ln(\phi_i^{\text{NE}}) = \left(\frac{\partial \tilde{a}^{\text{res,NE}}}{\partial s_i^{\text{NE}}} \right)_{T, s_{j \neq i}^{\text{NE}}} - \ln(Z^{\text{NE}}) \quad (13)$$

2.5. Phase-Equilibria

In order to describe the thermodynamic properties of a multicomponent single phase, Eq. 7,8,9 can be solved to calculate the compressibility Z , the density $\tilde{\rho}$ and the fugacity coefficient of each component ϕ_i as a function of temperature T , pressure p and the molar fraction of each component in the phase z_i . The calculation of the isothermal LVE for a multicomponent system is performed by including the previous calculation for both liquid and vapor phases inside a simple algorithm. According to this procedure, the temperature T and the composition in the liquid x_i are set to the desired values, while the pressure p and composition in the vapor y_i are calculated, by adding an equation for each component in order to account for the equilibrium between the liquid (L) and the vapor (V):

$$\phi_i^{\text{V}}(T, p, y_i) y_i = \phi_i^{\text{L}}(T, p, x_i) x_i \quad (14)$$

When considering multicomponent solubility in equilibrium systems such as rubbery polymers, the situation is the same, an external phase (E) with molar composition z_i (liquid x_i or vapor y_i) is in contact with a rubbery solid phase (S), leading to the following expression:

$$\phi_i^E(T, p, z_i) z_i = \phi_i^S(T, p, s_i) s_i \quad (15)$$

A similar expression holds true also when a generic external phase is in contact with a glassy polymeric phase. However, in this case, the fugacity of the non-equilibrium system becomes a function of the polymer density which substitute the equilibrium density calculated through the EOS in Eq. 15. According to this procedure, the temperature T , the pressure p , the molar fraction of each component in the external phase z_i , and the polymer density ρ_{pol} are typically set to desired values, while the molar fraction of each component in the glassy phase s_i is calculated, by adding an equation for each penetrant in order to account for the pseudo-equilibrium between the external phase (E) and the glassy phase (S):

$$\phi_i^E(T, p, z_i) z_i = \phi_i^{NE,S}(T, p, \rho_{pol}, s_i) s_i \quad (16)$$

2.6. Volume Additivity and Polymer Swelling

Considering a multicomponent mixture, it is possible to estimate the molar volume by using the assumption of volume additivity, through:

$$v_{mix} = \sum_i z_i v_i^0 \quad (17)$$

Where v_i^0 is the molar volume of the pure component i , at the same state, temperature and pressure of the mixture. According to this assumption, the volume calculated is an average of the volumes of the pure components, calculated on a molar basis. An equivalent expression for the specific volumes leads to:

$$\hat{v}_{mix} = \sum_i w_i \hat{v}_i^0 \quad (18)$$

Where \hat{v}_i^0 is the specific volume of the pure component i and w_i is the mass fraction of the component in the mixture. Eqs 17 and 18 can be used for fluid mixtures as well as polymer-solute systems under the assumption of zero or negligible excess volume in the mixture. Of course, for equilibrium systems such assumption can be removed if a EOS is available to describe the volumetric behavior of the mixture. For glassy polymers, on the other hand, this possibility is not available, so that, in the NET-GP approach, the assumption used to describe volume behavior upon mixing becomes an integral part of the modeling strategy. For the case of swelling penetrants, an external swelling law needs to be added in order to account for the reduction of the molar density of the polymer ρ_{pol} with respect to the one expected in the dry glass state $\rho_{pol,dry}$. A generic expression based on additive swelling behaviour [23] is used in this work for both liquid and vapor mixtures:

$$\rho_{pol} = \rho_{pol,dry} \left/ \left(1 + k_{sw} \right) = \rho_{pol,dry} \left/ \left(1 + \sum_i k_{sw,i} a_i^{\alpha_i} \right) \right. \quad (19)$$

Where k_{sw} is the overall swelling coefficient, $k_{sw,i}$ and α_i are the swelling coefficients of each penetrant i , and a_i is the activity of the penetrant i . The latter quantity is defined for each component in a generic mixture as its fugacity in the mixture f_i divided by its fugacity as pure component f_i^0 at the same state, temperature and pressure. It is noticed that the same expression holds, replacing molar density ρ with mass density $\hat{\rho}$ in Eq. 19.

2.7. Glass Transition Temperature

Before affording the calculation of the solubility isotherms of vapors and liquids in glassy polymers, it is required to check if the polymeric phase remains glassy in the overall activity range [46,64]. Indeed, a depression of the glass transition temperature can be expected, especially for highly soluble penetrants, before saturation. In the latter case, if the glass transition temperature of the system reaches the temperature of the isotherm, the glassy polymer phase becomes rubbery. As a

consequence, this needs to be accounted for in the calculation of the solubility, which can be done by using the equilibrium EoS, as well as the nonequilibrium approach, by using the same binary interaction parameter. By using this strategy, the glass transition should be localized at a certain point of the isotherm at which the equilibrium solubility is equal to the non-equilibrium one, due to the fact that the equilibrium density is exactly equal to the non-equilibrium one.

Another approach which can be used to validate the results of the solubility model is to use an empirical equation for the prediction of the glass transition depression. An expression widely used in the literature is the Kelley-Bueche equation [46,65]:

$$T_g = \frac{\phi_{sol} \alpha_{sol} T_{g,sol} + (1 - \phi_{sol}) \Delta \alpha_{pol} T_{g,pol}}{\phi_{sol} \alpha_{sol} + (1 - \phi_{sol}) \Delta \alpha_{pol}} \quad (22)$$

Where $T_{g,sol}$ and $T_{g,pol}$ are the glass transition temperatures of solute and polymer respectively, ϕ_{sol} is the volume fraction of the solute, α_{sol} is the thermal expansion coefficient of the solvent, and $\Delta \alpha_{pol}$ is the difference between the thermal expansion coefficient of the glassy and the rubbery phases of the polymer. Usually, ϕ_{sol} is estimated under the assumption of volumes' additivity, thus:

$$\phi_{sol} = \frac{s_{sol} v_{sol}}{s_{sol} v_{sol} + (1 - s_{sol}) v_{pol}} \quad (23)$$

Where v_{sol} and v_{pol} are the molar volumes of solute and polymer respectively. It is noticed that the same expression holds, replacing molar volumes v_i with specific volumes \hat{v}_i and molar fractions s_i with mass fractions w_i in Eq. 23.

3. Materials and Methods

In this section, the preparation of the samples and the experimental methods used to determine the multicomponent liquid solubility of acetone and methanol in Matrimid at 35°C and 1 bar are described, considering the gravimetric and the FTIR-ATR techniques.

3.1. Materials

Matrimid 5218 was purchased from Huntsman Advanced Materials in powder form, with an average molecular weight of 80000 g/mol, a polydispersity index of 4.5, and a glass transition temperature equal to 320°C [22]. All the samples were prepared as thin films by casting from a solution with dichloromethane (DCM) at 2% weight of Matrimid obtained by dispersing the polymer powder as received in the solvent, in a closed agitated vial overnight. In particular, the films for the gravimetric experiments were obtained by casting an adequate amount of the solution on a clean glass petri dish and allowing the solvent to evaporate, whereas in the case of the FTIR-ATR experiments, the polymer was cast directly onto the ATR crystal to ensure adhesion and avoid any defects at the polymer crystal interface which could compromise the sensitivity of the analysis. After the casting process, the membranes prepared were annealed under vacuum at about 200°C for 15 h to obtain homogeneous samples with a similar history and properties. The mass density of the samples was taken equal to 1.238 g/cm³, a reference value measured through Archimedes' principle, by weighing in air and in n-dodecane at 27°C [22]. Acetone and methanol were purchased from Sigma-Aldrich with reagent grade purity ($\geq 99.5\%$) and were used as received, without further purification. Five different liquid mixtures were prepared at ambient conditions upon mixing with different acetone molar fractions (0%, 25%, 50%, 75%, 100%) by weighting the proper amount of solvents by using an analytical balance, considering their molecular weight, equal to 32.04 g/mol for methanol and 58.08 g/mol for acetone. The relative uncertainty of the acetone molar fraction measured was $u_r(x_{Ac}) = 1.5\%$, as calculated as three times the accuracy of the instrument in the measurement of the mass, equal to $u_r(m) = 0.5\%$, considering the conversion from mass fraction to molar fraction. For the sake of

completeness, a sample provenance table, Table 2, is included in the text, which summarize the information reported above.

3.2. Gravimetric Measurements

In the gravimetric experiments, acetone and methanol liquid mixtures were deposited into different vials. The temperature of the vials was controlled by immersion in a thermostatic bath. The polymeric films prepared upon casting were weighted in the dry state and then immersed into the vials. At given time intervals the polymer samples were removed, quickly blotted, and weighted, until their mass reached a constant value at equilibrium m_{eq} . The total mass absorbed m_{abs} was then obtained as the difference between the total mass at equilibrium m_{eq} and the dry mass m_{dry} . The total mass ratio ω , expressed in grams of solvent per grams of polymer, is calculated as the total mass absorbed divided by the dry mass:

$$\omega = \frac{m_{abs}}{m_{dry}} = \frac{m_{eq} - m_{dry}}{m_{dry}} \quad (24)$$

Relative uncertainty of the measured solubility, $u_r(\omega)$, was estimated to be in the order of 1.5%, as calculated considering the errors of two equivalent measurements and the accuracy of the instrument.

3.3. FTIR-ATR Measurements

Attenuated total internal reflection (ATR) occurs when light propagates through a dense medium (ATR crystal) and is reflected at the interface with a rarer medium (polymer) [27]. In FTIR-ATR spectroscopy, an IR beam is generated from a source and modulated by an interferometer, to enter one side of the ATR crystal. The IR radiation reflects and absorbs at the crystal/polymer interface multiple times to finally exit from the opposite side of the crystal, to be quantified by a detector. At the interface, an exponentially decaying electromagnetic field (evanescent wave) propagates for a small distance, known as penetration depth, into the polymer, inducing a change in the IR absorbance of chemical bonds associated with the presence of solutes in the polymer or changes in the polymer due to molecular interactions with the solute. As a consequence, the absorbance, A , of the polymer and of the penetrant characteristic peaks can be used to study the concentration of the different components in the mixture. Indeed, a linear relationship between the integrated absorbance and molar concentration is usually existing as stated by the Beer-Lambert law [66]:

$$A_i = \varepsilon_i C_i \quad (25)$$

Where A_i is the integrated absorbance, C_i is the molar concentration, and ε_i is the molar extinction coefficient of the penetrant multiplied by the optical path traveled by the IR radiation. Eq. 25 can be rearranged for the penetrant related peaks in order to obtain an following expression:

$$A_i = \frac{\varepsilon_i \rho_{pol,dry}}{M_i} \frac{\omega_i}{(1 + k_{sw})} = \frac{K_i}{1 + k_{sw}} \omega_i \quad (26)$$

Where K_i is a constant (which depend on ε_i , molar mass of penetrant

M_i and density of the dry polymer $\rho_{pol,dry}$), ω_i is the mass ratio of component i (or solubility, expressed in g/g_{pol}) and k_{sw} is the overall swelling coefficient, which can be calculated by integrating the peaks associated to polymer swelling. Indeed in the sorption tests the number of the polymer chains present in the penetration depth of the IR beam a number which is decreasing due to swelling induced by the penetrant. Polymer peaks, proportional to polymer concentration in the matrix, can therefore be related to the swelling coefficient by using the following equation [30]:

$$k_{sw} = \frac{A_{p,dry} - A_{p,eq}}{A_{p,dry}} = \frac{A_{p,sw}}{A_{p,dry}} \quad (27)$$

Where $A_{p,eq}$ and $A_{p,dry}$ are the integrated absorbance of the polymer peak at equilibrium and dry condition respectively. The ATR crystal used in this work is based on zinc selenide (ZnSe), with a crystal angle equal to 45° and a refractive index of 2.6, higher than the one of the polymer, equal to 1.6. Characteristic peaks of the two acetone and methanol penetrants and the dry polymer Matrimid were determined by monitoring the absorbance peaks in the range 500-4000 cm⁻¹, in the pure liquid solvents and dry polymeric matrix cast on the ATR crystal, as shown in Fig. 1. Ideally, for each component, peaks must be selected, in the region where no absorbance is detected for the other two components. This was unfortunately not always possible in the present case so that the peaks with minimal interference were considered. In particular the peak selected for Matrimid corresponds to around 1300 cm⁻¹, the peak selected for acetone corresponds to around 1200 cm⁻¹, and the peak selected for methanol corresponds to around 3300 cm⁻¹.

Pure component sorption experiments were conducted by mounting the crystal cast with Matrimid in the ATR cell, measuring the initial absorbance in dry conditions related to the dry polymer peak $A_{p,dry}$ and the pure penetrant peak $A_{i,dry}$. Then, pure liquid solvents are put in contact with the polymer, and sorption starts, until the system reaches equilibrium. At this point, the absorbance related to the polymer peak at equilibrium $A_{p,eq}$ and the absorbance related to the pure penetrant peak at equilibrium $A_{i,eq}$ are measured.

The Matrimid swelling coefficient due to pure acetone sorption $k_{sw,Ac}$ was determined from the absorbance in the range between 1265 and 1315 cm⁻¹ which clearly decrease upon sorption as shown in Fig. 2a. The integrated absorbances of this peak in swollen condition (solid line in Fig. 2a) and dry condition (dotted line in Fig. 2a) were used as $A_{p,eq}$ and $A_{p,dry}$ in Eq. 27.

For acetone, the chosen peak was not affected by methanol presence but partially superimposed with the polymer peak centered at 1205 cm⁻¹. For this reason, in order to obtain the acetone concentration in the polymer, the overall absorbance in the region between 1175 and 1235 cm⁻¹ was corrected by subtracting the peak of dry Matrimid in that region rescaled trough Eq. 27 to account for swelling, as graphically shown in Fig. 2b. The same procedure was used also for the case of methanol whose main peak considered is the one related to -OH stretching which has been integrated between 3200 and 3600 cm⁻¹ where small absorbance peaks of both polymer and acetone are actually present. For this reason, the correction procedure was made considering not only the polymer swelling but also the acetone sorption when the latter was present in the mixture.

Once the pure penetrant absorbance, A_i^0 , for both acetone and methanol, were obtained from pure liquids sorption tests, they were used in Eq. 26 together with $k_{sw,i}$ and pure penetrant mass ratio obtained through gravimetric method ω_i^0 , to calculate the conversion constant K_i . In this way, from the pure component sorption data, all the information was retrieved to calculate the polymer swelling as well as the methanol and acetone concentration from absorbance peaks related to mixtures, which are shown in Fig. 3 for the wavenumber region of interest for polymer swelling (3a), acetone sorption (3b) and methanol sorption (3c) respectively.

In more detail, to calculate A_{Ac} , first, the swelling coefficient related

Table 2
Sample provenance table for the compounds used in this work.

Name	Acetone	Methanol	Matrimid 5218
IUPAC Name	2-Propanone	1-Methanol	Poly [3, 3', 4, 4'-benzophenone tetracarboxylic dianhydride and 5(6)-amino-1-(4'-aminophenyl-1, 3-trimethylindane)]
Source	Sigma-Aldrich	Sigma-Aldrich	Huntsman Advanced Materials
Formula	CH ₄ O	C ₃ H ₆ O	(C ₃₅ H ₂₄ N ₂ O ₅) _n
Purity (Mass)	≥99.5%	≥99.5%	-

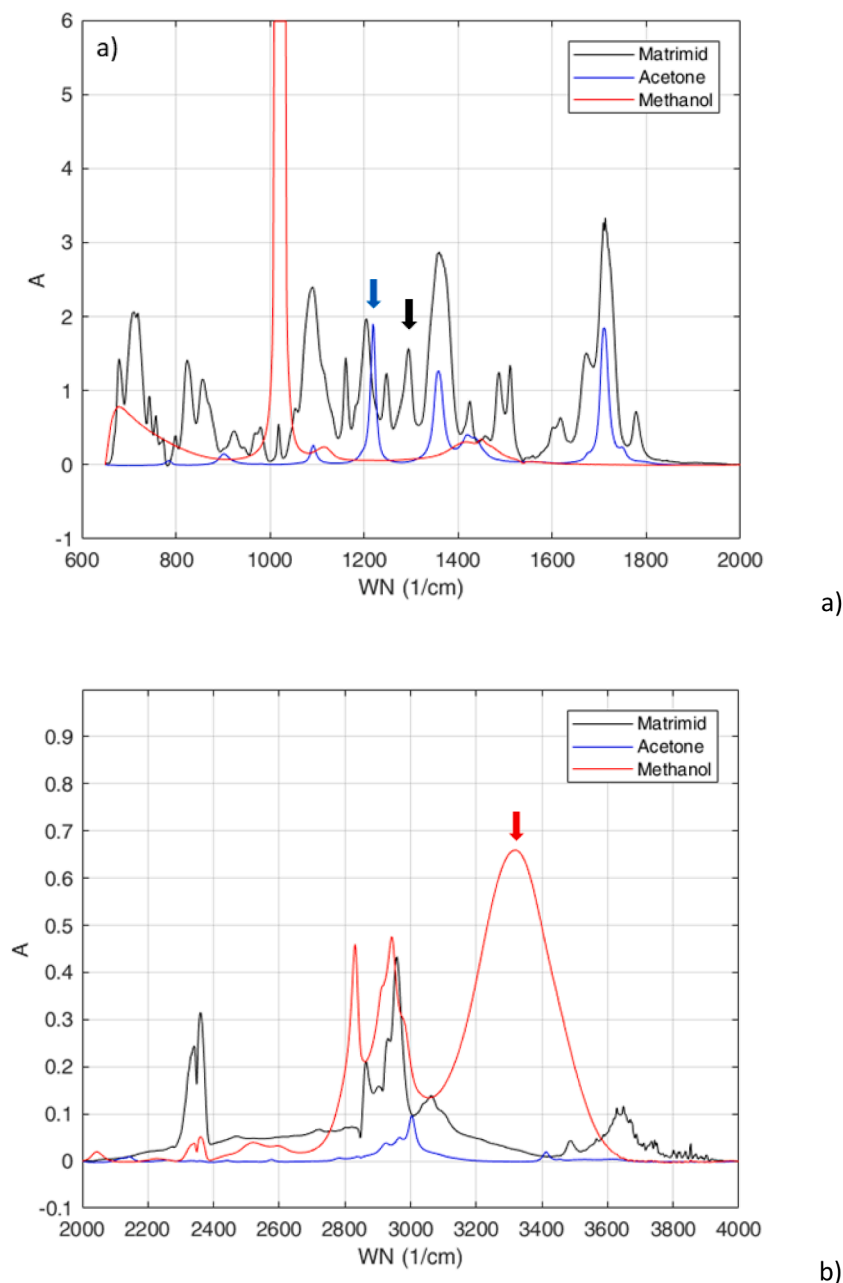


Fig. 1. Pure component absorbance peaks in the overall range inspected between 500 and 4000 cm^{-1} . a) characteristic peaks selected for Matrimid (black arrows) at around 1300 cm^{-1} , and acetone (blue arrows) at about 1200 cm^{-1} , and b) characteristic peak selected for methanol (red arrows) at 3300 cm^{-1} .

to multicomponent sorption $k_{sw, Ac}$ is calculated through Eq. 27, by using $A_{p,dry}$ and $A_{p,eq}$ calculated through numerical integration of the peak in the swelling range (1265-1315 cm^{-1}). Then, the contribution of the polymer absorbance in the acetone sorption range (1175-1235 cm^{-1}) related to swelling is calculated from the dry absorbance through Eq. 27 and subtracted to the overall equilibrium peaks, which are shown in Fig. 3b, to obtain the absorbance related to the sole acetone sorption. A similar procedure is then followed also for methanol, as the rescaled contribution of both the polymer and acetone peaks were subtracted from the overall absorbance in the region 3200-3600 cm^{-1} , to isolate the contribution of the sole methanol absorption.

In the case of multicomponent solubility, the relative uncertainty of the calculated values was 4.5%, considering the uncertainties of all the measurements. The relative uncertainty of the pure components solubility measured through gravimetric, $u_r(\omega^0)$, method was equal to 1.5%, as previously reported in section 3.2. The value of relative uncertainty

corresponding to the measured absorbance, $u_r(A)$, was calculated considering the maximum oscillation of the spectrum (observed in the acetone sorption region 1175-1235 cm^{-1}) leading to a value equal to 0.5%. The value of relative uncertainty corresponding to the measurement of the swelling coefficient $u_r(k_{sw})$ was calculated according to Eq. 27, as the double of $u_r(A)$, leading to a value equal to 1%. The value of relative uncertainty corresponding to the measurement of the constant K_i in Eq. 26, $u_r(K_i)$, was calculated according to Eq. 26, as the sum of $u_r(\omega^0)$, $u_r(A)$ and $u_r(k_{sw})$, leading to a value equal to 3%. Finally, the value of relative uncertainty corresponding to the measurement of the multicomponent solubility $u_r(\omega_i)$ was obtained according to Eq. 26, as the sum of $u_r(K_i)$, $u_r(A)$ and $u_r(k_{sw})$, leading to a value equal to 4.5%.

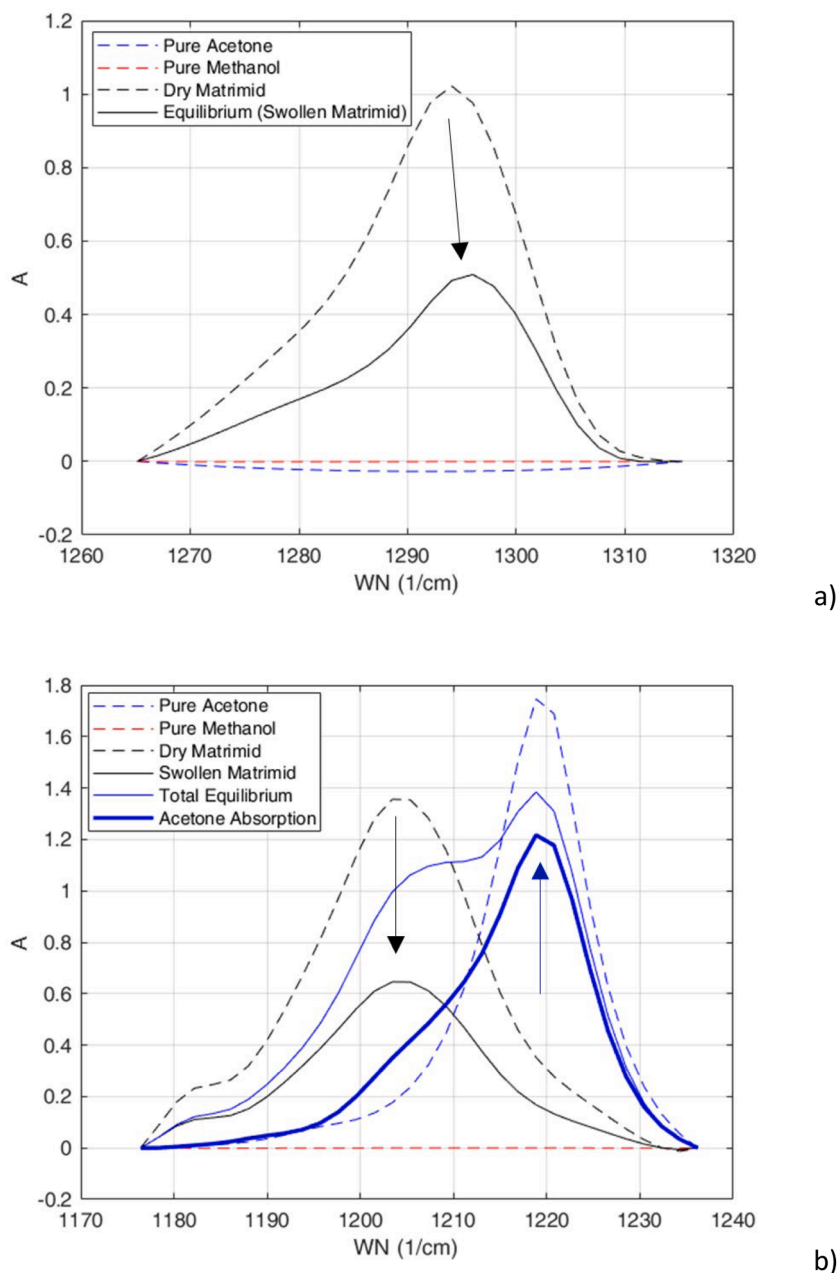


Fig. 2. Absorbance peaks detected for pure acetone sorption: a) Matrimid swelling peak between 1265 and 1315 cm^{-1} . b) Acetone sorption peak between 1175 and 1235 cm^{-1} .

4. Results and Discussion

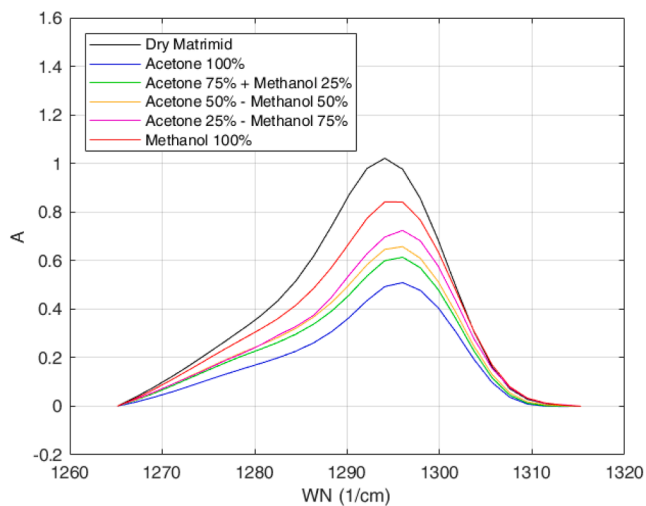
4.1. Pure Fluid Properties

The pure fluid parameters used in this work are reported in Table 1; they were selected from the cited literature and used to describe the thermodynamic properties of pure methanol and acetone. In order to check the reliability of the pure component parameters, the results are compared with thermodynamic properties of acetone and methanol reported in Perry's Chemical Engineering Handbook 8th edition [67].

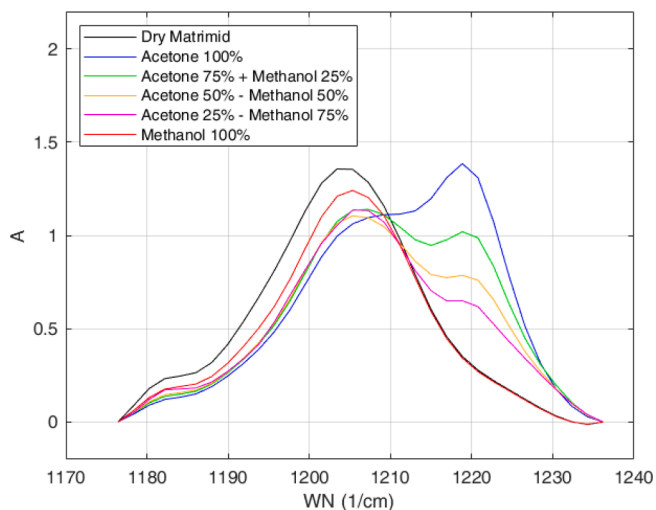
For the case of acetone, in particular, the model prediction in terms of vapor pressure and liquid and vapor saturated volumes as a function of temperature are shown in Fig. 4 and compared to the literature reference showing a very good agreement. In the following calculation, data for the pure component in the experimental condition (1 bar, 35°C) will be considered. In particular, the values needed are the vapor

pressure and the liquid density, which, for the case of acetone, are estimated to be equal to 0.459 bar at 35°C to 0.762 g/cm^3 respectively. The density of the liquid was calculated in the saturated condition but is almost equal to the one calculated for the liquid at 35°C and 1 bar, corresponding to a specific volume equal to 1.312 cm^3/g .

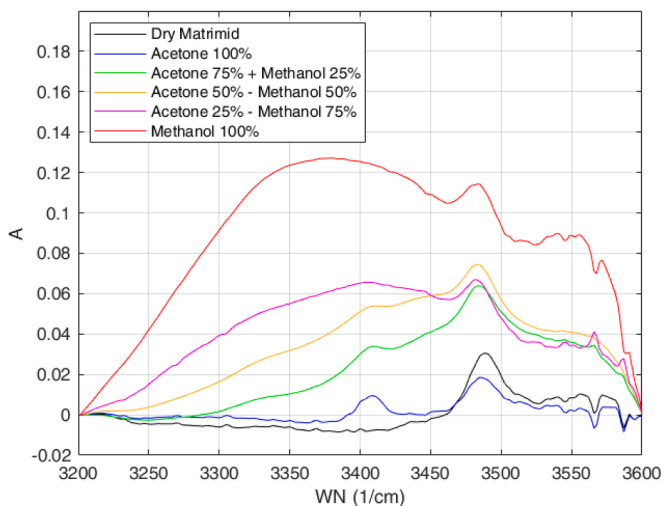
Similar results were obtained for the case of methanol: vapor pressure and liquid and vapor saturated volumes as a function of temperature are indeed well described by the model as shown in Fig. 5. As for acetone, the data used in the following modelling approach are the value of vapor pressure calculated at 35°C, equal to 0.270 bar, and the density of the liquid calculated in the saturated condition, equal to 0.767 g/cm^3 , again almost equal to the one calculated for the liquid at 35°C and 1 bar, corresponding to a specific volume equal to 1.304 cm^3/g .



a)



b)



c)

Fig. 3. Absorbance peaks detected for multicomponent sorption in the mixture at equilibrium: a) Matrimid swelling peak between 1265 and 1315 cm^{-1} ; b) Acetone sorption peak between 1175 and 1235 cm^{-1} ; c) Methanol sorption peak between 3200 and 3600 cm^{-1} .

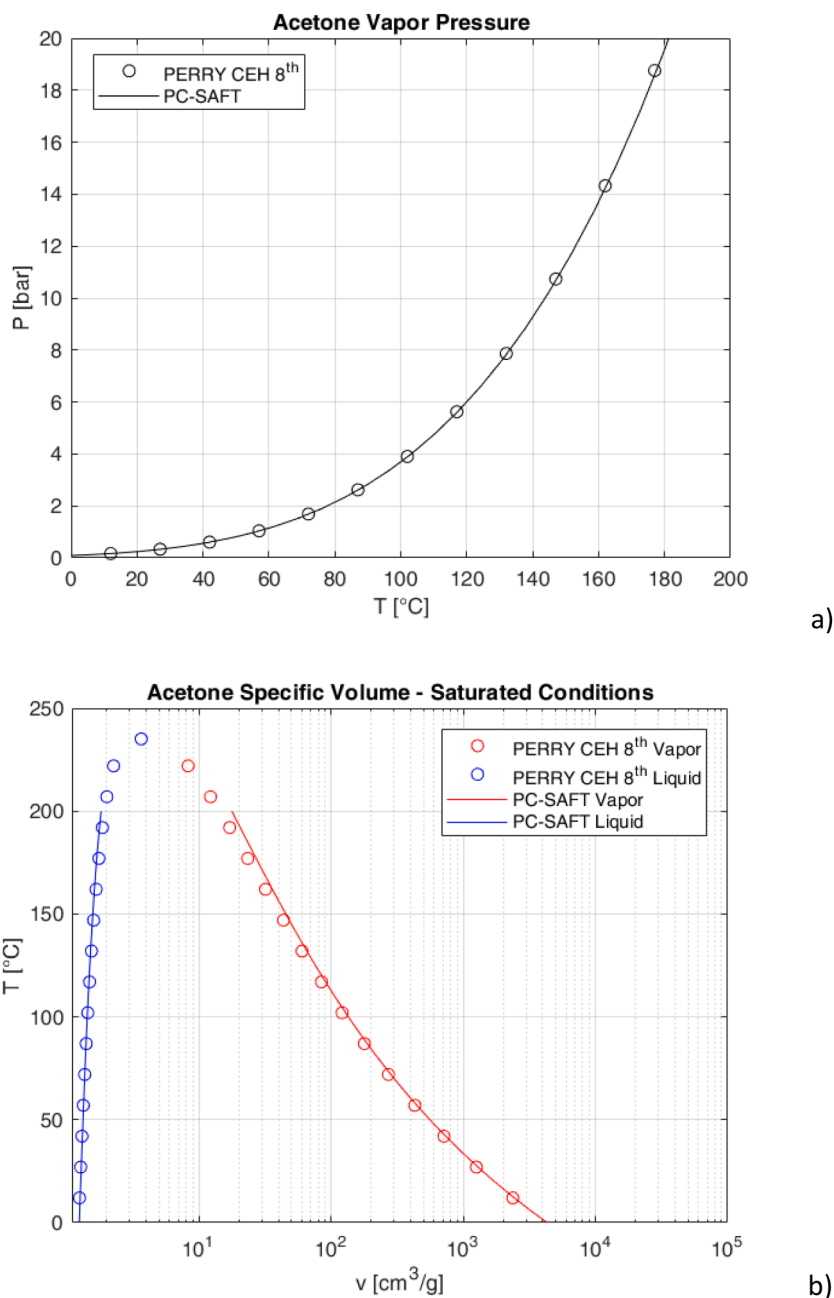


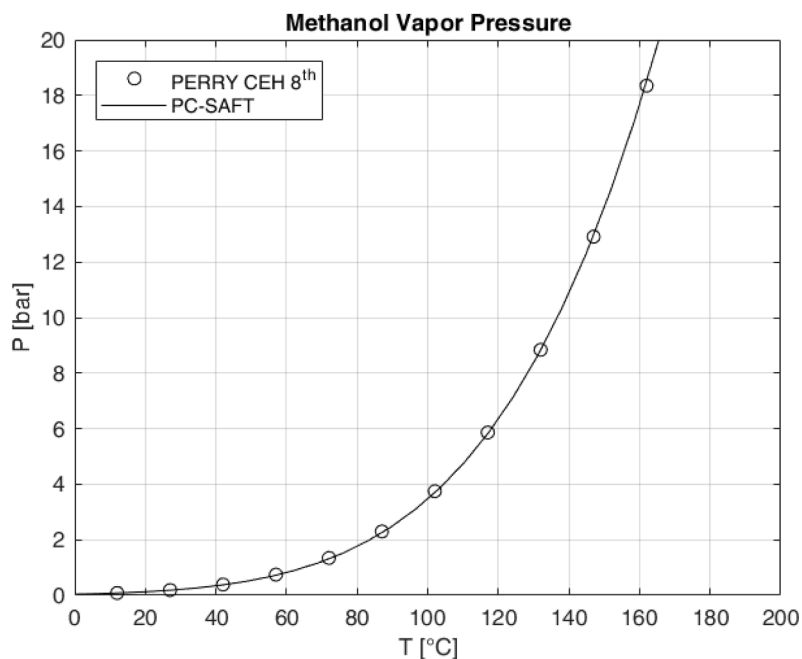
Fig. 4. PC-SAFT calculation of acetone vapor pressure (a) and liquid and vapor saturated volumes (b) as function of temperature is compared to literature reference [67].

4.2. Acetone-Methanol Binary System

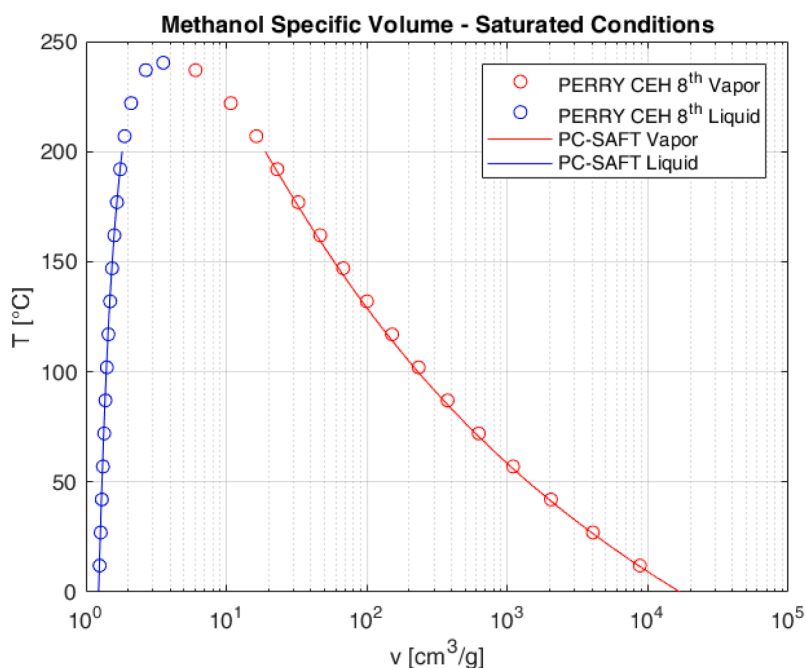
In order to obtain PC-SAFT binary interaction for the system acetone-methanol, liquid-vapor equilibrium data present in the open literature [57] were adopted as well as mixture molar volume [68], reported in Fig. 6a and 6b respectively. Pure components parameters reported in Table 1 were used and coupled with binary interaction parameters reported in Table 3, which were evaluated by fitting the isothermal LVE of the acetone-methanol binary system at 35°C by using PC-SAFT. As shown in Fig. 6a, by keeping the binary interaction coefficient $\nu_{ij} = 0$ and $k_{ij} = 0$, the PC-SAFT model predicts a positive deviation from ideality, but overestimates bubble and dew pressure of the mixture, with respect to the experimental reference. By using different values of binary interaction parameters, PC-SAFT is able to correctly describe experimental data. In particular, the binary interaction coefficient related to

the induced cross-association $\nu_{ij} = -0.24$ is higher in modulus than the one related to the interaction energy $k_{ij} = 0.01$. For the case of the acetone-methanol liquid mixture at 1 bar and 35°C, the molar volume as a function of the molar fraction of acetone is calculated, by using the same binary interaction coefficients reported in Table 3.

The result is shown in Fig. 6b and compared to the molar volume evaluated with the assumption of volume additivity (Eq. 17) and experimental reference [68]. From the figure, it can be seen that the PC-SAFT model is able to describe the deviation from the ideality, which brings the volume of the mixture to values slightly lower than the one calculated upon volume additivity. As a result, by mixing the two components at 35°C, the excess volume is slightly negative but substantially negligible.



a)



b)

Fig. 5. PC-SAFT calculation of methanol vapor pressure (a) and liquid and vapor saturated volumes (b) as function of temperature is compared to literature reference [67].

4.3. Acetone-Matrimid Binary System

For the case of the acetone-Matrimid system, the NET-GP approach is coupled with PC-SAFT in order to describe the vapor solubility isotherm at 35°C, as shown in Fig. 7a, in which the results are compared with experimental data already present in the open literature [22]. The use of the non-equilibrium approach in the whole concentration range was considered as the glass transition of the system at saturation estimated by the Kelley-Bueche model (Eq. 22,23), leads to $T_g = 46^\circ\text{C}$, well above the experimental one. For the estimation the following parameters were used as retrieved from the sorption isotherm and the relevant literature: $\omega_{Ac}^S = 0.32 \text{ g/g}_p$, $\Delta\alpha_p = 5 \times 10^{-4} \text{ 1/K}$ [18], $\alpha_s = 1.2 \cdot 10^{-3} \text{ 1/K}$ [67], $T_{g,p} =$

593 K [22] and $T_{g,s} = 100 \text{ K}$ [69].

The result of the approach is also reported in Fig. 7a, where it can be seen that the model underestimates the experimental data, when used without adjusting binary interaction correction ($k_{ij} = 0$, $\nu_{ij} = 0$) and swelling law ($k_{sw,i} = 0$, $\alpha_i = 0$). To correctly fit the sorption isotherm indeed $k_{sw,i} = 0.4164$ and $\alpha_i = 1$, are needed in Eq. 19, while both binary interaction coefficients, k_{ij} and ν_{ij} , remained equal to 0. In this case, therefore no binary interaction coefficients were needed, and this was attributed to the affinity between acetone and Matrimid repeating unit, due to the presence of carbonyl groups in both the two species. On the other hand, a linear swelling law was required, in order to correctly fit experimental data. In this concern, a strong swelling of the polymer

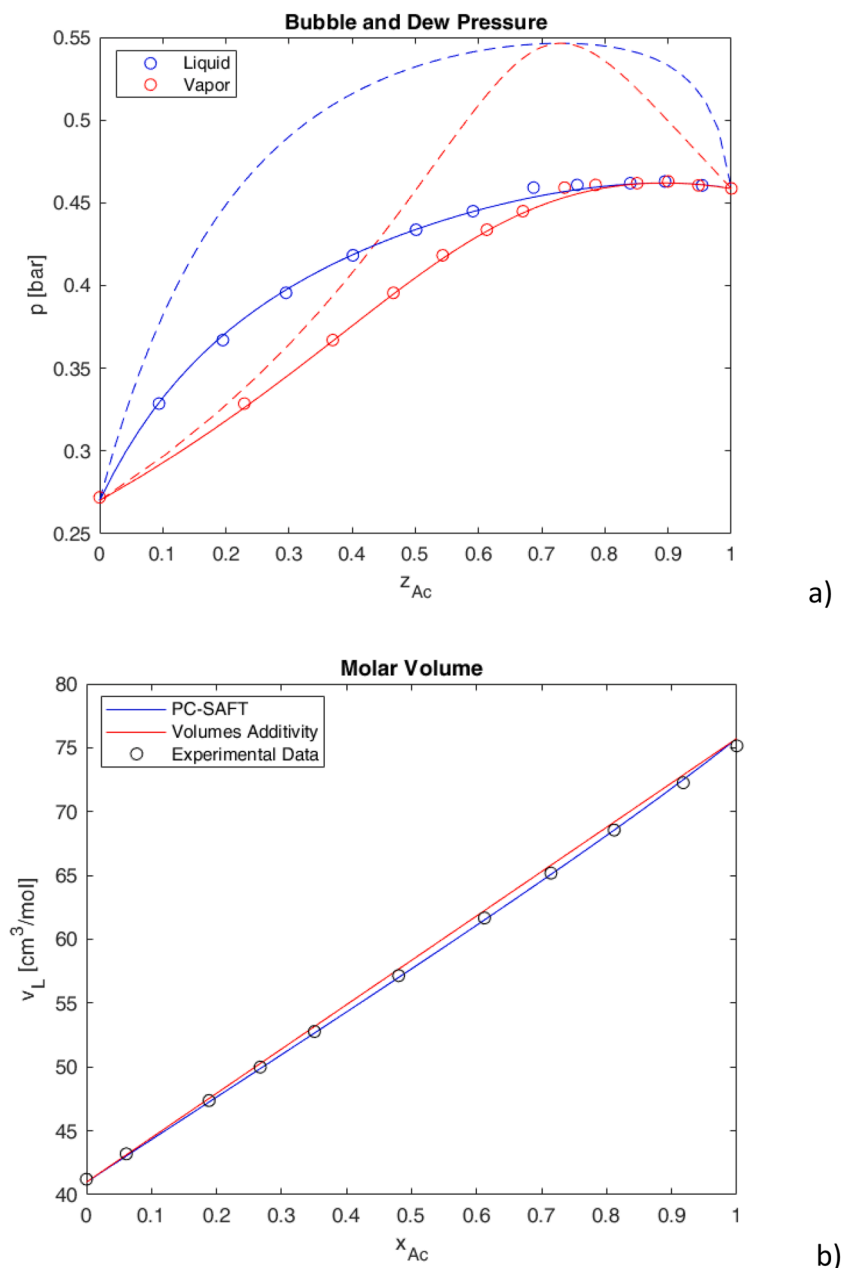


Fig. 6. a) PC-SAFT calculation of acetone-methanol isothermal LVE at 35°C, showing bubble pressure as a function of acetone liquid molar fraction (blue) and dew pressure as a function of acetone vapor molar fraction (red). The calculation with $k_{ij} = 0$ and $\nu_{ij} = 0$ (dashed lines) is compared with the calculation corrected with $k_{ij} = 0.01$ and $\nu_{ij} = -0.24$ (solid lines) and with experimental data (colored dots) [57]. b) PC-SAFT calculation of acetone-methanol mixture liquid molar volume at 1 bar and 35°C (blue line) is compared to the calculation made through Eq. 17 under the assumption of volume additivity (red line), and the experimental data (black dots) [68].

Table 3

PC-SAFT binary interaction parameters and swelling coefficients used in this work, in order to fit experimental data of binary systems.

i	j	k_{ij}	ν_{ij}	$k_{sw,i}$	α_i
Acetone	Methanol	0.01	-0.24	-	-
Acetone	Matrimid	0	0	0.4164	1
Methanol	Matrimid	-0.07	0	0.1527	3

matrix is observed in Fig. 7b due to acetone sorption. Calculated density indeed evolve from the dry polymer density (1.238 g/cm³) to a value of 0.875 g/cm³ at saturation, corresponding to 41.64% swelling, a value slightly lower than one measured by Kappert *et al.* at 22°C, equal to

around 55% [8]. The solubility calculated at saturation without considering swelling is equal to $w_{Ac}^S = 0.06$ g/g_P, a value 5 times lower than the solubility calculated at saturation considering swelling which is equal to $w_{Ac}^S = 0.32$ g/g_P. It is noticed that a similar result was obtained by using the Sanchez and Lacombe Lattice Fluid (LF) model [22] as reference EOS for the NET-GP approach, with $k_{ij} = 0.0035$ and $k_{sw,1} = 0.4131$, confirming that no association is needed to describe this system.

In the figures also results from the equilibrium PC-SAFT are reported. In this case, the solubility predicted is always lower than experimental data, meaning that the system remains glassy in the overall activity range. The results, indeed, become very similar to the experimental ones, only close to saturation. From this point of view therefore the EOS suggest that in this condition the polymer is close to the glass transition,

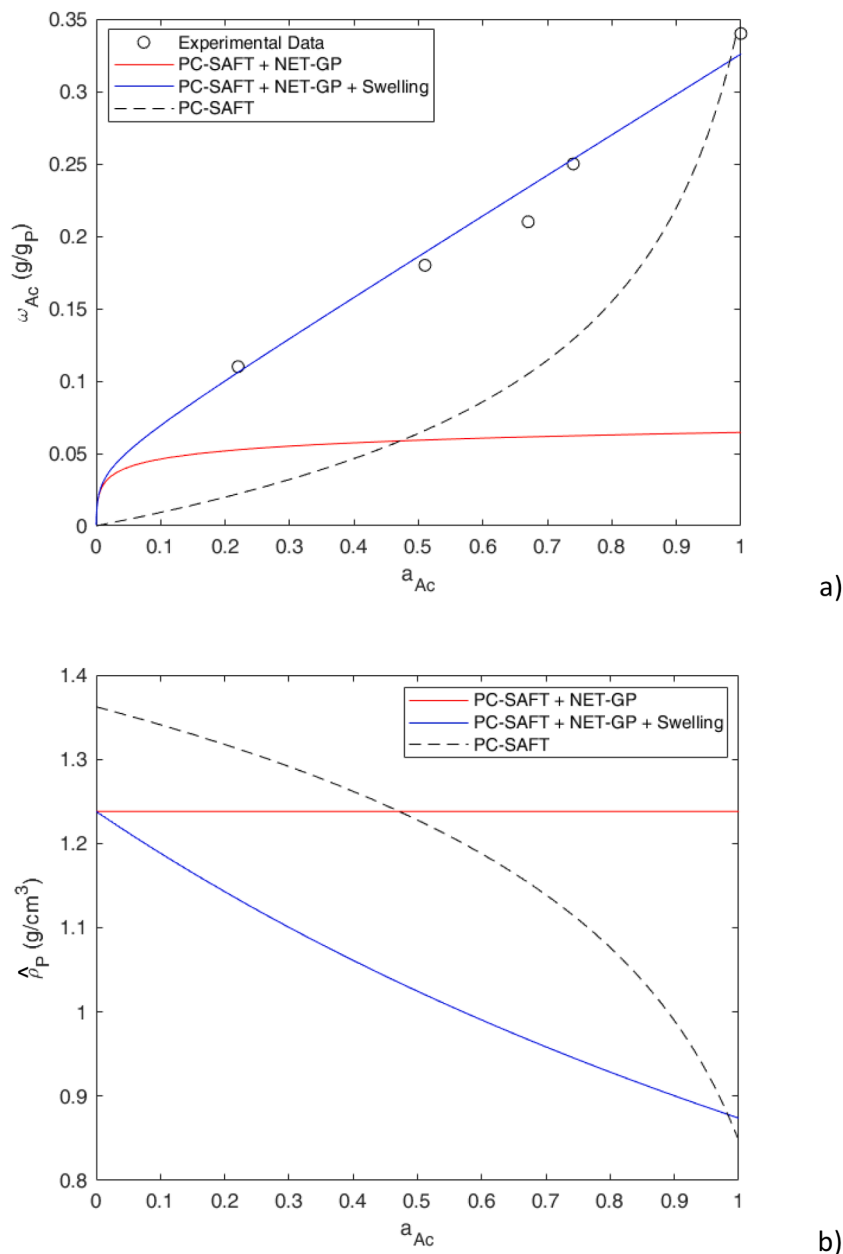


Fig. 7. a) NET-GP + PC-SAFT calculation of acetone solubility in Matrimid at 35°C, in terms of mass ratio (grams of acetone divided by grams of polymers) as a function of acetone activity. The calculation with $k_{ij} = 0, \nu_{ij} = 0, k_{sw,i} = 0, \alpha_i = 0$ (red line) is compared with the calculation corrected with $k_{sw,i} = 0.4164, \alpha_i = 1$ (blue line) to represent experimental data (black dots) [22]. b) Polymer mass density as a function of acetone activity (blue line) is compared to dry polymer density (red line). For the sake of completeness, also the calculation at equilibrium with PC-SAFT (dashed line) is shown, for both solubility and polymer density at equilibrium.

which therefore results lower than the one calculated by Kelley-Bueche model. Also in this case the results are similar to what obtained in a previous work by using LF model [22].

4.4. Methanol-Matrimid Binary System

For the case of the methanol-Matrimid system, the calculation of the vapor solubility isotherm at 35°C by coupling NET-GP with PC-SAFT is shown in Fig. 8a fitted to experimental data available from previous work [22]. Also in this case indeed it is noticed that the glass transition of the system at saturation, estimated by using $\omega_{Me}^S = 0.17$ g/g_P, $\Delta\alpha_p = 5 \times 10^{-4}$ 1/K [18], $\alpha_s = 1.2 \cdot 10^{-3}$ 1/K [67], $T_{g,p} = 593$ K [22] and $T_{g,s} = 100$ K [69] in the Kelley-Bueche model (Eq. 22,23), lead to a value of 124°C, well above the experimental temperature.

In this case, binary interaction correction ($k_{ij} = -0.07, \nu_{ij} = 0$) was required in order to describe low activity data, by assuming no swelling ($k_{sw,i} = 0, \alpha_i = 0$), while in order to describe the entire isotherm, a cubic swelling law was required, by using $k_{sw,1} = 0.1527$ and $\alpha_i = 3$ in Eq. 19. Therefore, only one binary interaction coefficient was used, and this was attributed to the difference between methanol and Matrimid repeating units due to the presence of different groups in the two species. According to the results shown in Fig. 8b, a lower swelling was observed with respect to acetone. In particular, polymer mass density reduced up to 1.075 g/cm³ at saturation, corresponding to 15.27% swelling, a value slightly below the value measured by Kappert *et al.* at 22°C, equal to around 25% [8]. As a consequence, the solubility calculated at saturation without considering swelling is equal to $\omega_{Me}^S = 0.06$ g/g_P, a value 3 times lower than the solubility calculated at saturation considering

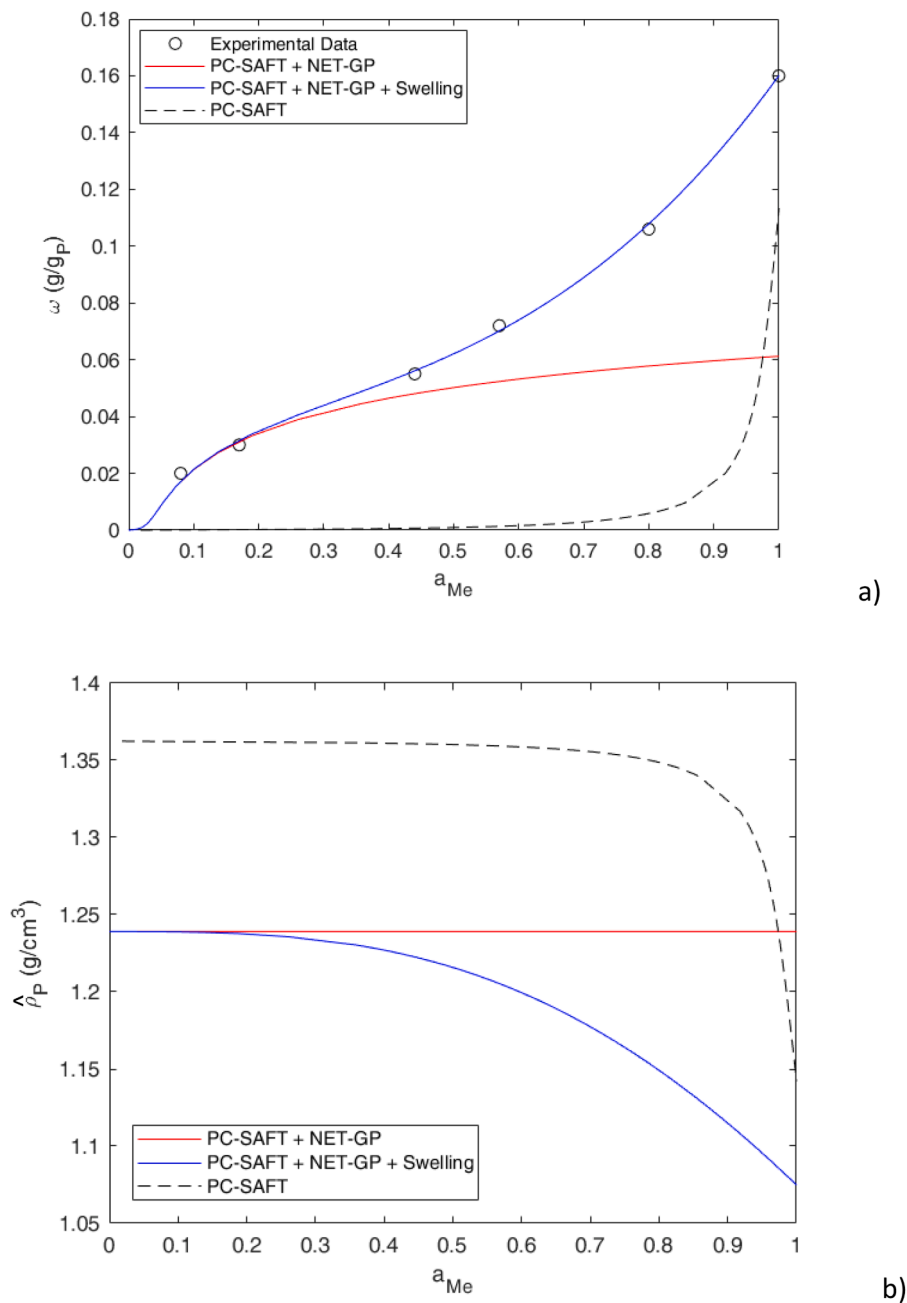


Fig. 8. a) NET-GP + PC-SAFT calculation of methanol solubility in Matrimid at 35°C, in terms of mass ratio (grams of acetone divided by grams of polymers), as a function of methanol activity. The calculation with $k_{ij} = -0.07$, $\nu_{ij} = 0$, $k_{sw,i} = 0$, $\alpha_i = 0$ (red line) is compared with the calculation corrected with $k_{sw,i} = 1527$, $\alpha_i = 3$ (blue line) to represent experimental data (black dots) [22]. b) Polymer mass density as a function of acetone activity (blue line) is compared to dry polymer density (red line). For the sake of completeness, also the calculation at equilibrium with PC-SAFT (dashed line) is shown, for both solubility and polymer density at equilibrium.

swelling, equal to $\omega_{Me}^S = 0.17$ g/g_p. It is noticed that, without considering the swelling, the solubility at saturation of both the two solvents is equal to 0.06 g/g_p, as the solvents are virtually occupying all the free volume of the dry polymer, with the same mass. It is indeed the swelling caused by the penetrants that dominate the sorption behaviour, with respect to the interactions between penetrants and polymer.

Once again the obtained results are similar to those obtained by using LF as reference EOS for the NET-GP approach in terms of binary interaction coefficient, equal to $k_{ij} = -0.035$, even if a different swelling law with two parameters was required for methanol [22]. A substantial difference between the two modelling approaches can be observed in the low activity region near zero. In particular,

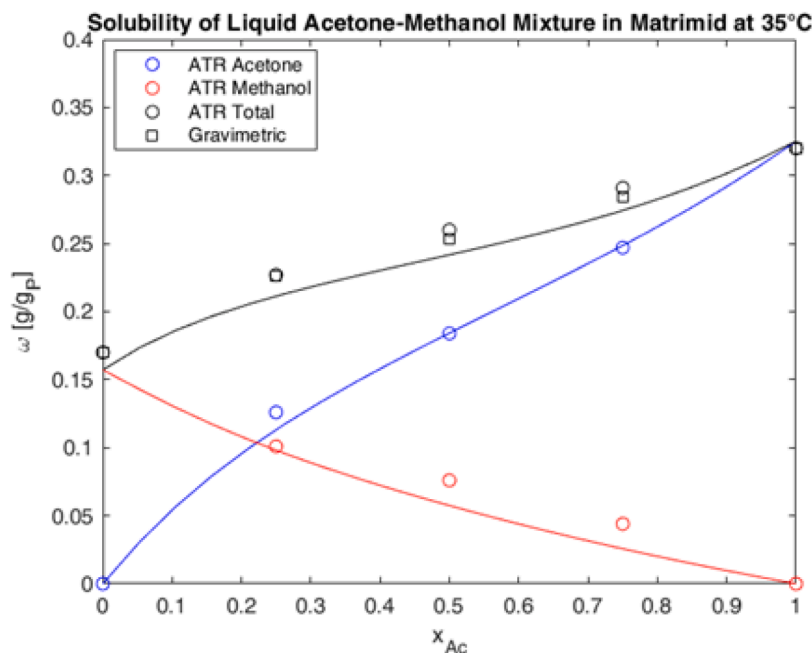
methanol-methanol associations modelled through PC-SAFT result in an upward concavity which was not visible by using LF that does not allow to account for associations [22]. For the same reason, also the PC-SAFT equilibrium calculation is affected by hydrogen bonds at high activities, leading to a much higher upward concavity with respect to the one calculated with LF. This latter result may also derive from the simplification made in order to represent methanol association, by using the 2B scheme. As previously observed for acetone, the system remains glassy in the overall activity range, but again the difference between equilibrium and non-equilibrium decreases close to saturation.

4.5. Acetone-Methanol-Matrimid Ternary System

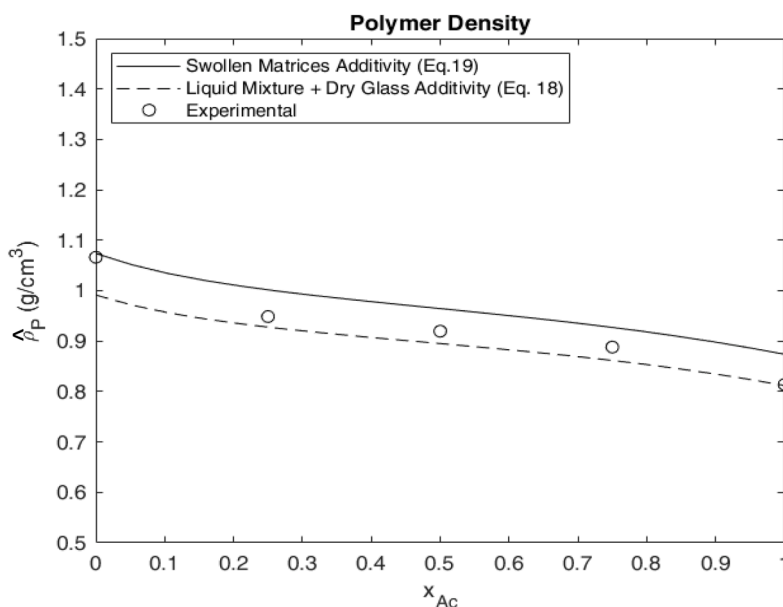
Experimental data of the Acetone-Methanol-Matrimid ternary system at 35°C are shown in Figs. 9a and 9b, referring respectively to sorption data, taken by ATR and gravimetric analysis, and to swelling data as obtained from ATR analysis. According to the values reported in Table 4, the total solvent solubility, as the sum of methanol and acetone, obtained from ATR measurement (ω_{ATR}) agrees with the total solubility obtained through gravimetric method (ω_{GR}), with a relative error always lower than 1%. The overall swelling coefficient measured through ATR (k_{sw}), reported in Table 4, increases with acetone molar fraction in the liquid phase, going from pure methanol (16.1%) to pure acetone

(52.1%). The values obtained are once again comparable to the ones measured by Kappert *et al.* at 22°C [8], equal to around 25% and 55% for methanol and acetone respectively, and with the one obtained by fitting pure vapors isotherms with the model proposed, respectively equal to 15.27% and 41.64%.

In the same figure also the modelling results are represented in terms of solubility and swelling. The system is described by using the NET-GP approach based on PC-SAFT, using pure component parameters reported in Table 1 and binary coefficients reported in Table 3. For liquid sorption, the density of the swollen polymer used as the internal state variable of the ternary system is calculated through Eq.19. This assumption, made to obtain a complete prediction of the ternary sorption data, led to



a)



b)

Fig. 9. a) Solubility (ω) of acetone (blue) and methanol (red) in Matrimid as a function of acetone molar fraction in the binary liquid mixture (x_{Ac}): the results predicted with NET-GP + PC-SAFT (solid lines) are compared with the experimental data obtained through FTIR-ATR technique (dots) and the ones measured and gravimetric method (squares). b) Polymer dilation as a function of acetone molar fraction: the density of the polymer obtained experimentally through ATR (dots) is compared with the density of the polymer calculated with Eq. 18, under the assumption of volume additivity between the dry glass and the liquid mixture (dotted line) and the density of the polymer calculated through Eq. 19, the swelling law which was used for the calculation of the solubility (solid line).

Table 4

Experimental data obtained in this work for the acetone and methanol liquid mixture sorption in Matrimid and polymer dilation at $T = 35^\circ$.

x_{Ac}	0.000	0.250	0.500	0.750	1.000
k_{sw}	0.161	0.305	0.346	0.394	0.521
ω_{Ac}	0.000	0.127	0.183	0.244	0.320*
ω_{Me}	0.170*	0.104	0.076	0.044	0.000
ω_{ATR}	0.170*	0.230	0.259	0.288	0.320*
ω_{GR}	0.170*	0.226*	0.253*	0.284*	0.320*

Standard relative uncertainties u_r are $u_r(T) = 0.3\%$, $u_r(x_{Ac}) = 1.5\%$, $u_r(k_{sw}) = 1\%$, $u_r(\omega^*) = 1.5\%$, $u_r(\omega) = 4.5\%$. *Obtained from gravimetric (GR) measurement.

a substantial agreement between the experimental results and the modelling. As visible in Fig. 9a, indeed, the solubility of each component in the glass predicted with NET-GP and PC-SAFT by using Eq. 19 as swelling law agrees with the experimental data obtained through FTIR-ATR and gravimetric method, which are reported in Table 4. In particular, while acetone was very well described by the model, higher relative errors, up to 20%, were observed in the prediction of methanol solubility, with a maximum for the mixture with 75% acetone molar fraction. Nonetheless, the prediction of total solvent solubility was more than satisfactory as the relative errors between prediction (black line in Fig. 9a) and experimental data (black dots in Fig. 9a) were always lower than 5%. Indeed, the high errors related to methanol sorption had only a slight influence in the prediction of overall solvent uptake as they refer to conditions where methanol sorption is less than one third of the acetone one, as clearly visible from Fig. 9a.

Also, the description of the density resulted in line with experimental data obtained through FTIR-ATR analysis or calculated through volume additivity (Eq. 18) which are both shown in Fig. 9b together with the one used for solubility calculation (Eq. 19). The latter values are in general slightly higher than the one obtained through volume additivity, with maximum deviation in the order of 10%. The experimental data, on the other hand, always remain inside the two calculated data set. Interestingly, the fact that experimental dilation is slightly higher than the one obtained through Eq. 19, is coherent with the slight underestimation of the sorption isotherm made by the model. In general, however, the results confirm the agreement between experimental data and the model also in the description of polymer dilation upon sorption.

Therefore, the method proposed confirms to be suitable to fully predict multicomponent liquid solubility by using binary coefficients obtained through pure component sorption, and a simple mixing ruled for volumes that do not introduce any additional coefficients.

5. Conclusions

The PC-SAFT equation of state was coupled with the NET-GP approach in order to predict liquid-solid equilibrium of the ternary system Matrimid/Methanol/Acetone based on a set of data obtained by coupling ATR-FTIR analysis with gravimetric tests. Initially, the PC-SAFT was used to correctly describe the isothermal VLE of the acetone-methanol mixture at 35°C , thus obtaining information about the binary interaction parameters related to this mixture. Binary parameters for the solvent-polymer mixtures were then obtained by coupling the NET-GP approach with the PC-SAFT to fit the solubility isotherms of pure acetone and methanol in Matrimid at 35°C . In particular for each binary system, interaction parameters as well as swelling coefficients were retrieved upon experimental data fitting, which always resulted in a very good agreement between data and modeling results.

Finally the modelling approach was extended to ternary system without any additional parameters and used to describe the experimental data, related to Matrimid/Methanol/Acetone at 35°C and 1 bar, in terms of both composition and density. The results were very good,

the overall sorption isotherm was slightly underestimated by the model likely due to an overestimation of the mixing rule for density calculation. The predicted density resulted indeed slightly higher than the experimental one thus underestimating the degree of swelling of the polymer. Interestingly then the model was able to correctly describe also the behavior of Methanol and Acetone concentration in the polymer as a function of the external activity. In this concern, therefore, NET GP approach confirmed its potential as a tool to describe also liquid solvent equilibrium in glassy polymer, once it is coupled with a reliable equation of state as PC-SAFT proved to be in the present case.

CRedit authorship contribution statement

Lorenzo Merlonghi: Writing – review & editing, Writing – original draft, Methodology, Investigation, Data curation, Conceptualization. **Ferruccio Doghieri:** Writing – review & editing, Supervision, Formal analysis, Conceptualization. **Marco Giacinti Baschetti:** Writing – review & editing, Supervision, Methodology, Formal analysis, Data curation, Conceptualization.

Declaration of competing interest

The authors declare that they have no known competing financial interests or personal relationships that could have appeared to influence the work reported in this paper.

Data availability

Data will be made available on request.

References

- [1] J.G. (Hans) Wijmans, R.W. Baker, The solution–Diffusion Model: A unified approach to membrane permeation, in: Y. Yampolskii, I. Pinnau, B. Freeman (Eds.), *Materials Science of Membranes for Gas and Vapor Separation*, 1st ed., Wiley, 2006, pp. 159–189, <https://doi.org/10.1002/047002903X.ch5>. Eds.
- [2] 1st ed S. Matteucci, Y. Yampolskii, B.D. Freeman, I. Pinnau, Transport of gases and vapors in glassy and rubbery polymers, in: Y. Yampolskii, I. Pinnau, B. Freeman (Eds.), *Materials Science of Membranes for Gas and Vapor Separation*, Wiley, 2006, pp. 1–47, <https://doi.org/10.1002/047002903X.ch1>, 1st ed.
- [3] B. Adhikari, S. Majumdar, Polymers in sensor applications, *Progress in Polymer Science* 29 (7) (Jul. 2004) 699–766, <https://doi.org/10.1016/j.progpolymsci.2004.03.002>.
- [4] J.W. Grate, M.H. Abraham, Solubility interactions and the design of chemically selective sorbent coatings for chemical sensors and arrays, *Sensors and Actuators B: Chemical* 3 (2) (Feb. 1991) 85–111, [https://doi.org/10.1016/0925-4005\(91\)80202-U](https://doi.org/10.1016/0925-4005(91)80202-U).
- [5] M.A. Del Nobile, G. Mensitieri, C. Manfredi, A. Arpaia, L. Nicolais, Low molecular weight molecules diffusion in advanced polymers for food packaging applications, *Polym. Adv. Technol.* 7 (5–6) (May 1996) 409–417, [https://doi.org/10.1002/\(SICI\)1099-1581\(199605\)7:5<409::AID-PAT501>3.0.CO;2-M](https://doi.org/10.1002/(SICI)1099-1581(199605)7:5<409::AID-PAT501>3.0.CO;2-M).
- [6] P. Masi, D.R. Paul, Modeling gas transport in packaging applications, *Journal of Membrane Science* 12 (2) (Dec. 1982) 137–151, [https://doi.org/10.1016/S0376-7388\(00\)80178-7](https://doi.org/10.1016/S0376-7388(00)80178-7).
- [7] B. Seifert, et al., Polyetherimide: A new membrane-forming polymer for biomedical applications, *Artificial Organs* 26 (2) (Feb. 2002) 189–199, <https://doi.org/10.1046/j.1525-1594.2002.06876.x>.
- [8] E.J. Kappert, M.J.T. Raaijmakers, K. Tempelman, F.P. Cuperus, W. Ogieglo, N. E. Benes, Swelling of 9 polymers commonly employed for solvent-resistant nanofiltration membranes: A comprehensive dataset, *Journal of Membrane Science* 569 (Jan. 2019) 177–199, <https://doi.org/10.1016/j.memsci.2018.09.059>.
- [9] R.W. Baker, K. Lokhandwala, Natural gas processing with membranes: an overview, *Ind. Eng. Chem. Res.* 47 (7) (Apr. 2008) 2109–2121, <https://doi.org/10.1021/ie071083w>.
- [10] L.S. White, T.A. Blinka, H.A. Kloczewski, I. Wang, Properties of a polyimide gas separation membrane in natural gas streams, *Journal of Membrane Science* 103 (1–2) (Jul. 1995) 73–82, [https://doi.org/10.1016/0376-7388\(94\)00313-N](https://doi.org/10.1016/0376-7388(94)00313-N).
- [11] L. Wang, Y. Cao, M. Zhou, Q. Liu, X. Ding, Q. Yuan, Gas transport properties of 6FDA-TMPDA/MOCA copolyimides, *European Polymer Journal* 44 (1) (Jan. 2008) 225–232, <https://doi.org/10.1016/j.eurpolymj.2007.10.021>.
- [12] R. Recio, et al., Gas separation of 6FDA–6FpDA membranes Effect of the solvent on polymer surfaces and permselectivity, *Journal of Membrane Science* 293 (1–2) (Apr. 2007) 22–28, <https://doi.org/10.1016/j.memsci.2007.01.022>.
- [13] S. Shishatskiy, C. Nistor, M. Popa, S.P. Nunes, K.V. Peinemann, Polyimide asymmetric membranes for hydrogen separation: influence of formation conditions

- on gas transport properties, *Adv Eng Mater* 8 (5) (May 2006) 390–397, <https://doi.org/10.1002/adem.200600024>.
- [14] C.A. Scholes, W.X. Tao, G.W. Stevens, S.E. Kentish, Sorption of methane, nitrogen, carbon dioxide, and water in Matrimid 5218, *J of Applied Polymer Sci* 117 (4) (Aug. 2010) 2284–2289, <https://doi.org/10.1002/app.32148>.
- [15] K. Vanherck, P. Vandezande, S.O. Aldea, I.F.J. Vankelecom, Cross-linked polyimide membranes for solvent resistant nanofiltration in aprotic solvents, *Journal of Membrane Science* 320 (1–2) (Jul. 2008) 468–476, <https://doi.org/10.1016/j.memsci.2008.04.026>.
- [16] Y.H. See-Toh, F.C. Ferreira, A.G. Livingston, The influence of membrane formation parameters on the functional performance of organic solvent nanofiltration membranes, *Journal of Membrane Science* 299 (1–2) (Aug. 2007) 236–250, <https://doi.org/10.1016/j.memsci.2007.04.047>.
- [17] J. Crank, *The mathematics of diffusion*, Clarendon Press Oxford, 1957.
- [18] D. W. Van Krevelen and K. Te Nijenhuis, *Properties of polymers: their correlation with chemical structure; their numerical estimation and prediction from additive group contributions*. 2009.
- [19] R.K. Arya, D. Thapliyal, J. Sharma, G.D. Verros, Glassy polymers—Diffusion, sorption, ageing and applications, *Coatings* 11 (9) (Aug. 2021) 1049, <https://doi.org/10.3390/coatings11091049>.
- [20] D. Pierleoni, 'Novel experimental methods and modeling of solvent induced glass transition and structural relaxation in polymers', 2018, doi: 10.6092/UNIBO/AMSDOTTORATO/8671.
- [21] E. Piccinini, M. Giacinti Baschetti, G.C. Sarti, Use of an automated spring balance for the simultaneous measurement of sorption and swelling in polymeric films, *Journal of Membrane Science* 234 (1–2) (May 2004) 95–100, <https://doi.org/10.1016/j.memsci.2003.12.024>.
- [22] M. Minelli, G. Cocchi, L. Ansaloni, M.G. Baschetti, M.G. De Angelis, F. Doghieri, Vapor and liquid sorption in matrimid polyimide: experimental characterization and modeling, *Ind. Eng. Chem. Res.* 52 (26) (Jul. 2013) 8936–8945, <https://doi.org/10.1021/ie3027873>.
- [23] E. Ricci, F.M. Benedetti, A. Noto, T.C. Merkel, J. Jin, M.G. De Angelis, Enabling experimental characterization and prediction of ternary mixed-gas sorption in polymers: C₂H₆/CO₂/CH₄ in PIM-1, *Chemical Engineering Journal* 426 (Dec. 2021) 130715, <https://doi.org/10.1016/j.cej.2021.130715>.
- [24] E. Ricci, et al., Sorption of CO₂/CH₄ mixtures in TZ-PIM, PIM-1 and PTMSP: experimental data and NELF-model analysis of competitive sorption and selectivity in mixed gases, *Journal of Membrane Science* 585 (Sep. 2019) 136–149, <https://doi.org/10.1016/j.memsci.2019.05.026>.
- [25] O. Vopička, M.G. De Angelis, G.C. Sarti, Mixed gas sorption in glassy polymeric membranes: I. CO₂/CH₄ and n-C₄/CH₄ mixtures sorption in poly(1-trimethylsilyl-1-propyne) (PTMSP), *Journal of Membrane Science* 449 (Jan. 2014) 97–108, <https://doi.org/10.1016/j.memsci.2013.06.065>.
- [26] E.S. Sanders, W.J. Koros, H.B. Hopfenberg, V.T. Stannett, Mixed gas sorption in glassy polymers: equipment design considerations and preliminary results, *Journal of Membrane Science* 13 (2) (Apr. 1983) 161–174, [https://doi.org/10.1016/S0376-7388\(00\)80159-3](https://doi.org/10.1016/S0376-7388(00)80159-3).
- [27] Y.A. Elabd, M.G. Baschetti, T.A. Barbari, Time-resolved Fourier transform infrared/attenuated total reflection spectroscopy for the measurement of molecular diffusion in polymers, *J Polym Sci B Polym Phys* 41 (22) (Nov. 2003) 2794–2807, <https://doi.org/10.1002/polb.10661>.
- [28] V. Loianno, A. Baldanza, G. Scherillo, P. Musto, G. Mensitieri, Sorption of CO₂, CH₄ and their mixtures in amorphous poly(2,6-dimethyl-1,4-phenylene)oxide (PPO), *Polymers* 15 (5) (Feb. 2023) 1144, <https://doi.org/10.3390/polym15051144>.
- [29] A. Pereira, M. Lopes, J. Timmer, J. Keurentjes, Solvent sorption measurements in polymeric membranes with ATR-IR spectroscopy, *Journal of Membrane Science* 260 (1–2) (Sep. 2005) 174–180, <https://doi.org/10.1016/j.memsci.2005.03.041>.
- [30] M. Giacinti Baschetti, E. Piccinini, T.A. Barbari, G.C. Sarti, Quantitative analysis of polymer dilution during sorption using FTIR-ATR spectroscopy, *Macromolecules* 36 (25) (Dec. 2003) 9574–9584, <https://doi.org/10.1021/ma0302457>.
- [31] P.J. Flory, Thermodynamics of high polymer solutions, *The Journal of Chemical Physics* 10 (1) (Jan. 1942) 51–61, <https://doi.org/10.1063/1.1723621>.
- [32] P.J. Flory, Thermodynamics of dilute solutions of high polymers, *The Journal of Chemical Physics* 13 (11) (Nov. 1945) 453–465, <https://doi.org/10.1063/1.1723978>.
- [33] R.H. Lacombe, I.C. Sanchez, Statistical thermodynamics of fluid mixtures, *J. Phys. Chem.* 80 (23) (Nov. 1976) 2568–2580, <https://doi.org/10.1021/j100564a009>.
- [34] I.C. Sanchez, R.H. Lacombe, An elementary molecular theory of classical fluids. Pure fluids, *J. Phys. Chem.* 80 (21) (Oct. 1976) 2352–2362, <https://doi.org/10.1021/j100562a008>.
- [35] I.C. Sanchez, R.H. Lacombe, Statistical thermodynamics of polymer solutions, *Macromolecules* 11 (6) (Nov. 1978) 1145–1156, <https://doi.org/10.1021/ma60066a017>.
- [36] I.C. Sanchez, P.A. Rodgers, Solubility of gases in polymers, *Pure and Applied Chemistry* 62 (11) (Jan. 1990) 2107–2114, <https://doi.org/10.1351/pac199062112107>.
- [37] W.G. Chapman, K.E. Gubbins, G. Jackson, M. Radosz, SAFT: equation-of-state solution model for associating fluids, *Fluid Phase Equilibria* 52 (Dec. 1989) 31–38, [https://doi.org/10.1016/0378-3812\(89\)80308-5](https://doi.org/10.1016/0378-3812(89)80308-5).
- [38] W.G. Chapman, K.E. Gubbins, G. Jackson, M. Radosz, New reference equation of state for associating liquids, *Ind. Eng. Chem. Res.* 29 (8) (Aug. 1990) 1709–1721, <https://doi.org/10.1021/ie00104a021>.
- [39] S. Kanehashi, K. Nagai, Analysis of dual-mode model parameters for gas sorption in glassy polymers, *Journal of Membrane Science* 253 (1–2) (May 2005) 117–138, <https://doi.org/10.1016/j.memsci.2005.01.003>.
- [40] E. Ricci, M. De Angelis, Modelling mixed-gas sorption in glassy polymers for CO₂ removal: A sensitivity analysis of the dual mode sorption model, *Membranes* 9 (1) (Jan. 2019) 8, <https://doi.org/10.3390/membranes9010008>.
- [41] F. Doghieri, G.C. Sarti, Nonequilibrium lattice fluids: A predictive model for the solubility in glassy polymers, *Macromolecules* 29 (24) (Jan. 1996) 7885–7896, <https://doi.org/10.1021/ma951366c>.
- [42] G.C. Sarti, F. Doghieri, Predictions of the solubility of gases in glassy polymers based on the NELF model, *Chemical Engineering Science* 53 (19) (Oct. 1998) 3435–3447, [https://doi.org/10.1016/S0009-2509\(98\)00143-2](https://doi.org/10.1016/S0009-2509(98)00143-2).
- [43] M.G. Baschetti, F. Doghieri, G.C. Sarti, Solubility in glassy polymers: correlations through the nonequilibrium lattice fluid model, *Ind. Eng. Chem. Res.* 40 (14) (Jul. 2001) 3027–3037, <https://doi.org/10.1021/ie000834q>.
- [44] F. Doghieri, M.G. De Angelis, M.G. Baschetti, G.C. Sarti, Solubility of gases and vapors in glassy polymers modelled through non-equilibrium PHSC theory, *Fluid Phase Equilibria* 241 (1–2) (Mar. 2006) 300–307, <https://doi.org/10.1016/j.fluid.2005.12.040>.
- [45] M.G. De Angelis, F. Doghieri, G.C. Sarti, B.D. Freeman, Modeling gas sorption in amorphous Teflon through the non equilibrium thermodynamics for glassy polymers (NET-GP) approach, *Desalination* 193 (1–3) (May 2006) 82–89, <https://doi.org/10.1016/j.desal.2005.06.057>.
- [46] G.C. Sarti, M.G. De Angelis, Calculation of the solubility of liquid solutes in glassy polymers, *AIChE Journal* 58 (1) (Jan. 2012) 292–301, <https://doi.org/10.1002/aic.12571>.
- [47] F. Doghieri, pVT data analysis for the prediction of vapor sorption in glassy polymers through the nonequilibrium PC-SAFT model, *J. Chem. Eng. Data* 69 (2) (Feb. 2024) 538–559, <https://doi.org/10.1021/acs.jced.3c00441>.
- [48] E. Ricci, M. Minelli, M.G. De Angelis, A multiscale approach to predict the mixed gas separation performance of glassy polymeric membranes for CO₂ capture: the case of CO₂/CH₄ mixture in Matrimid®, *Journal of Membrane Science* 539 (Oct. 2017) 88–100, <https://doi.org/10.1016/j.memsci.2017.05.068>.
- [49] J. Gross, G. Sadowski, Modeling polymer systems using the perturbed-chain statistical associating fluid theory equation of State, *Ind. Eng. Chem. Res.* 41 (5) (Mar. 2002) 1084–1093, <https://doi.org/10.1021/ie010449g>.
- [50] L. Hesse, G. Sadowski, Modeling liquid–Liquid equilibria of polyimide solutions, *Ind. Eng. Chem. Res.* 51 (1) (Jan. 2012) 539–546, <https://doi.org/10.1021/ie201114z>.
- [51] E. Ricci, et al., Towards a systematic determination of multicomponent gas separation with membranes: the case of CO₂/CH₄ in cellulose acetates, *Journal of Membrane Science* 628 (Jun. 2021) 119226, <https://doi.org/10.1016/j.memsci.2021.119226>.
- [52] B.D. Marshall, R. Mathias, R.P. Lively, B.A. McCool, Theoretically self-consistent nonequilibrium thermodynamics of glassy polymer theory for the solubility of vapors and liquids in glassy polymers, *Ind. Eng. Chem. Res.* 60 (36) (Sep. 2021) 13377–13387, <https://doi.org/10.1021/acs.iecr.1c02194>.
- [53] B.D. Marshall, W. Li, R.P. Lively, Dry glass reference perturbation theory predictions of the temperature and pressure dependent separations of complex liquid mixtures using SBAD-1 glassy polymer membranes, *Membranes* 12 (7) (Jul. 2022) 705, <https://doi.org/10.3390/membranes12070705>.
- [54] J. Gross, G. Sadowski, Application of perturbation theory to a hard-chain reference fluid: an equation of state for square-well chains, *Fluid Phase Equilibria* 168 (2) (Feb. 2000) 183–199, [https://doi.org/10.1016/S0378-3812\(00\)00302-2](https://doi.org/10.1016/S0378-3812(00)00302-2).
- [55] J. Gross, G. Sadowski, Application of the perturbed-chain SAFT equation of State to associating systems, *Ind. Eng. Chem. Res.* 41 (22) (Oct. 2002) 5510–5515, <https://doi.org/10.1021/ie010954d>.
- [56] J. Gross, G. Sadowski, Perturbed-chain SAFT: an equation of State based on a perturbation theory for chain molecules, *Ind. Eng. Chem. Res.* 40 (4) (Feb. 2001) 1244–1260, <https://doi.org/10.1021/ie0003887>.
- [57] A.N. Marinichev, M.P. Susarev, *J. Appl. Chem. USSR, JAPUAW* 38 (1965) 371–375, 2.
- [58] I.D. Gil, D.C. Botía, P. Ortiz, O.F. Sánchez, Extractive distillation of acetone/methanol mixture using water as entrainer, *Ind. Eng. Chem. Res.* 48 (10) (May 2009) 4858–4865, <https://doi.org/10.1021/ie801637h>.
- [59] Graczoza Elena, Vavrusova Monika, Extractive distillation of acetone methanol mixture using 1-ethyl-3-methylimidazolium trifluoromethanesulfonate, *Chemical Engineering Transactions* 70 (2018) 1189–1194, <https://doi.org/10.3303/CET1870199>.
- [60] G. Modla, P. Lang, Separation of an acetone–methanol mixture by pressure-swing batch distillation in a double-column system with and without thermal integration, *Ind. Eng. Chem. Res.* 49 (8) (Apr. 2010) 3785–3793, <https://doi.org/10.1021/ie901935z>.
- [61] I.A. Kouskoumvekaki, N. Von Solms, M.L. Michelsen, G.M. Kontogeorgis, Application of the perturbed chain SAFT equation of state to complex polymer systems using simplified mixing rules, *Fluid Phase Equilibria* 215 (1) (Jan. 2004) 71–78, [https://doi.org/10.1016/S0378-3812\(03\)00363-7](https://doi.org/10.1016/S0378-3812(03)00363-7).
- [62] M. Kleiner, G. Sadowski, Modeling of polar systems using PC-SAFT: an approach to account for induced-association interactions, *J. Phys. Chem. C* 111 (43) (Nov. 2007) 15544–15553, <https://doi.org/10.1021/jp072640v>.
- [63] J.P. Wolbach, S.I. Sandler, Using molecular orbital calculations to describe the phase behavior of cross-associating mixtures, *Ind. Eng. Chem. Res.* 37 (8) (Aug. 1998) 2917–2928, <https://doi.org/10.1021/ie970781i>.
- [64] G. Cocchi, M.G. Baschetti, M.G. De Angelis, F. Doghieri, Solubility of dichloromethane in Matrimid® 5218: measurement and modelling through the non equilibrium thermodynamics of glassy polymer (Net-gp) approach, *Procedia Engineering* 44 (2012) 1739–1740, <https://doi.org/10.1016/j.proeng.2012.08.930>.

- [65] F.N. Kelley, F. Bueche, Viscosity and glass temperature relations for polymer-diluent systems, *J. Polym. Sci.* 50 (154) (Apr. 1961) 549–556, <https://doi.org/10.1002/pol.1961.1205015421>.
- [66] D.F. Swinehart, The Beer-Lambert Law, *J. Chem. Educ.* 39 (7) (Jul. 1962) 333, <https://doi.org/10.1021/ed039p333>.
- [67] R.H. Perry, D.W. Green, *Perry's Chemical Engineers' Handbook*, 2007.
- [68] S.A. Levichev, A. Rusanov, Surface tension, density, and excess volumina in binary and ternary solutions. *Surface Tension, Density, and Excess Volumina in Binary and Ternary Solutions*, *Fiziko-chimiceskie Svoystva rastvorov*, Leningrad, 1964, pp. 219–226.
- [69] C.A. Angell, J.M. Sare, E.J. Sare, Glass transition temperatures for simple molecular liquids and their binary solutions, *J. Phys. Chem.* 82 (24) (Nov. 1978) 2622–2629, <https://doi.org/10.1021/j100513a016>.